

**Temperature window for encapsulation of enzymes into thermally shrunk, CaCO<sub>3</sub> templated polyelectrolyte multilayer capsules**

Louis Van der Meeren\*, Jie Li, Manfred Konrad, Andre G. Skirtach, Dmitry Volodkin, Bogdan V. Parakhonskiy

Ir. L. Van der Meeren, J. Li, Prof. Dr. A.G. Skirtach, Dr. B. V. Parakhonskiy  
Department of Biotechnology, Ghent University, 9000 Ghent, Belgium  
E-mail: Louis.VanderMeeren@UGent.be

Dr. M. Konrad  
Max Planck Institute for Biophysical Chemistry, 37077 Göttingen, Germany

Prof. D. Volodkin  
School of Science and Technology, Nottingham Trent University, Nottingham NG11 8NS,  
U.K.

**Keywords:** enzymes, encapsulation, temperature, Layer-by-Layer, capsules

**Abstract.** Encapsulation of enzymes allows to preserve their biological activities in various environmental conditions, such as exposure to elevated temperature or to proteases. This is particularly relevant for in-vivo applications, where proteases represent a severe obstacle to maintaining the activity of enzymes. One type of drug delivery carriers suitable for enzyme encapsulation is polyelectrolyte multilayer capsules, and one of the most popular ways for encapsulation is based on hard templating using CaCO<sub>3</sub>. In this work, we encapsulate an active enzyme, ALP (alkaline phosphatase, involved in metabolism and skeletal development), into thermally shrunk polyelectrolyte multilayer (PDADMAC/PSS)<sub>4</sub> capsules (average diameter of 3.56 μm) templated on CaCO<sub>3</sub> microparticles and study activity of the encapsulated enzymes. At the optimal temperature for encapsulation (42°C), activity of the enzyme is almost four times higher than that at 30°C or 50°C. Retention of the enzyme activity has been assessed and the evolution of capsule size and density has been monitored *in situ* using fluorescence and atomic force microscopic techniques.

## Introduction

Encapsulation of enzymes is important for biochemistry to enable *in-vivo* applications. Polyelectrolyte multilayer (PEM) capsules represent some of the best suited types of delivery vehicles; they are assembled by sequential coating of sacrificial templates with polymeric layers and subsequently dissolving of the template leaving an empty polymeric shell (capsule). Multifunctionality, versatility and stimuli-responsiveness<sup>[1]</sup> make PEM capsules unique drug delivery carriers. PEM capsules are particularly suited for enzyme encapsulation<sup>[2-7]</sup> (please remove ref. 4) due to the properties of the polymeric shell – i.e. permeability to ions, which are used to dissolve the template, as well as to small molecules, which can serve as substrates for the enzyme. The capsules can effectively preserve and host rather large organic molecules, such as peptides, proteins, and even active enzymes. Such capsules are becoming important drug delivery carriers and they have been shown to carry essential functionality in regard with preserving the activity of enzymes against proteases.<sup>[8]</sup>

Various methods are available for fabrication of PEM microcapsules<sup>[9,10]</sup> and many of these are suitable for encapsulation of enzymes<sup>[11]</sup> – this application is seen as one of the most extensive applications of microcapsules. Another interesting feature of PEM microcapsules is that enzymatic reactions can be monitored by fluorescence microscopy,<sup>[12]</sup> and this can be carried out with sensoric functions, which have been recently classified,<sup>[13]</sup> as was shown for a sensor detecting urea.<sup>[14]</sup> Microcapsules have been designed for use in diverse areas of bio-medical applications<sup>[15]</sup> and sensorics,<sup>[16]</sup> and elaborate enzymatically controlled reactions have been monitored,<sup>[17]</sup> including those in multicompartments<sup>[18]</sup> capsules.<sup>[19]</sup> Both synthetic and biodegradable polymers can be employed for constructing the PEM shell of the capsules. The polymers can be used for initiating<sup>[20]</sup> or controlling<sup>[21]</sup> the release rate from microcapsules, and for preserving enzymes for biological applications.

Among different encapsulation strategies, heat treatment is a very promising method, because the size and mechanical properties of such capsules<sup>[22]</sup> and planar layers<sup>[23,24]</sup> can be

controlled. In regard with sacrificial particles serving as templates on which polyelectrolyte multilayers are deposited, vaterite  $\text{CaCO}_3$  particles are seen as one of the most promising candidates due to their bio-friendliness and inexpensiveness. Enzymes can effectively be encapsulated into the  $\text{CaCO}_3$  vaterite particles being loaded at extremely high concentrations (tens of mM) keeping their bioactivity which is mainly affected by pH value during enzyme loading (*10.1016/j.matdes.2019.108223*; *10.1016/j.colsurfb.2019.05.077*). The co-synthesis is nowadays one of the most effective methods to load molecules of various nature including proteins, polysaccharides and also small drugs (*10.1016/j.matdes.2019.108020*; *10.1016/j.jcis.2019.03.042*; *10.1039/c7cp07836f*). Thermal shrinking has been implemented on small calcium carbonate particles<sup>[26–28]</sup>. In addition, the main question expected for thermal encapsulation of enzymes -how enzymatic activity will be affected by temperature variation- is still unanswered.

In this work, we have encapsulated an active enzyme, ALP (alkaline phosphatase), into thermally shrunk microcapsules templated on  $\text{CaCO}_3$  particles. In situ fluorescence microscopy is used to trace the shrinking process of microcapsules, while Atomic Force Microscope (AFM) is used to study them in the pre- and post- shrunk states. Furthermore, enzymatic activity is analysed for free (not encapsulated) enzymes and at various temperatures up to  $60^\circ\text{C}$  upon thermally based encapsulation. The best temperature or thermal “window” for encapsulation and preservation of catalytic activity of enzymes is identified to be just above the glass transition temperature of polyelectrolyte pair constituting the shell.

### **Increasing temperature leads to capsule shrinkage**

The schematics of experiments on thermal encapsulation is depicted in Figure 1. In order to assess the size of capsule shrinkage over the course of heating the particles, tetramethyl-rhodamine-iso-thiocyanate (TRITC) linked to bovine serum albumin (BSA) is inserted during fabrication of the capsules, thus allowing to precisely determine the capsules diameter using

fluorescence microscopy. Initially, the capsules were heated in multiple steps to the (maximum) temperature of 60°C. At each of these steps, the diameters of multiple capsules were measured (Figure 2A). It looks that BSA is distributed rather homogeneously inside the capsules indicating its high loading inside. Such capsules having a very high content of proteins and polymers inside may serve as mimics of a biological cell (*10.1021/acs.langmuir.8b04328*).

Due to the polydispersity of the capsules, the extent of the diameter change of microcapsules was chosen as a measure of their shrinkage. During the heating process the diameter shrinks gradually (Figure 2B). When 60°C is reached the capsules have shrunk on average to 70% of their original diameter. Moreover, when these capsules were cooled down to 30 degrees, no significant difference in volume change was observed (Figure 2C). Since these polymers have a glass transition temperature at ~ 40°C, determined by differential scanning calorimetry,<sup>[29]</sup> heating the capsules above this temperature allows reorganisation of polymers accompanied with the size reduction of PEM microcapsules. The glass transition temperature depends on the polyelectrolyte polymers, water molecules,<sup>[30,31]</sup> complexation of polymers,<sup>[32]</sup> and salt ions<sup>[33]</sup> in the solution. Temperature can affect the structure of both as-prepared multilayers and also growing ones (*10.1039/c6cp00345a*).

AFM also allows morphological characterization. In this case it is interesting to look how shrinkage influences the density of capsules after drying. To measure this parameter, the ratio of surface area over volume was calculated. An example of the typical morphology of dried capsules before and after shrinking is shown in Figure 3A. Data of this experiment revealed that for the heated shrunk particles the density of the shell-forming polymers is significantly higher (Figure 3B). Therefore, the ratio of area over height is smaller for the heated capsules by the factor of six, as it is seen from Figure 3C. It should be noted that silica templated capsules appear much flatter<sup>[34]</sup> in comparison to those templated on calcium carbonate (Figure 3A), which is consistent with very different mechanical response of silica<sup>[35]</sup> templated versus calcium carbonate<sup>[36]</sup> templated capsules

**Temperature dependent shrinkage increases the encapsulation efficiency**

To test how the heat-induced shrinkage process can be used to encapsulate enzyme, an activity assay was performed with ALP. To determine the amount of active ALP in the capsules, an enzyme activity standard curve for increasing concentrations of ALP was set-up at multiple temperatures (Figure S1, Supporting Information). This allowed to analyse the inactivation of free ALP at increasing temperatures (Figure 4 A). These data showed (orange bars in Figure 1 B) a decreasing activity of the enzyme to 67, 33 and 18% upon heating for 1 hour at 40, 50 and 60°C, respectively. The grey part of the bars in Figure 4 B represent enzymes deactivated by the thermal treatment. The degradation rate has a linear dependence on the temperature ( $R^2 = 0.99957$ ), the degradation coefficient is  $-0.01667$  mg/mL active ALP per increased degree. These experiments served as a control for monitoring the activity of enzymes encapsulated into thermally shrunk microcapsules.

Subsequently, capsules were heated to the same temperatures in the presence of ALP, which was allowed to penetrate inside capsules. The schematics of these experiments showing details of this process are depicted in Figure 4 C. After heating, the capsules were centrifuged, and ALP activity was assessed in the capsules (Figure 4 E). Interestingly, when looking at the percentage of active and encapsulated ALP (Figure 4 E), the values are higher at 40°C and 50°C compared to that at 30°C. When combining these data with previously made observation that capsules shrink at elevated temperatures (Figure 2), it shows that by shrinking one can effectively reach a higher concentration of ALP inside capsules. The most attractive temperature (in terms of encapsulation efficiency and enzyme performance) is found to be 42°C (Figure 4 E). At this and slightly higher (several degrees) temperatures, a high percentage of encapsulated ALP can be achieved. In comparison to activity of enzymes exposed to 30°C or encapsulated at 50°C, the activity of enzymes encapsulated at 42°C is found to be approximately four times higher (Figure 4 E). As it was mentioned above, 42°C degree

represents temperature that lies just above the glass transition temperature ( $\sim 40^\circ\text{C}$ ) of the used polyelectrolyte pair (PDADMAC/PSS). At temperatures below  $40^\circ\text{C}$ , these polyelectrolytes assembled in a multilayer are situated still in a “glassy” state, i.e. no encapsulation takes place, while at higher temperature ( $50^\circ\text{C}$  and higher) although activity is higher (yellow curve in Figure 4D), the overall activity of all enzymes is decreasing (blue line in Figure 4 D).

At  $30^\circ\text{C}$  almost no shrinkage takes place, as it can be also concluded from previous experiments and at  $60^\circ\text{C}$  extensive inactivation has occurred. Considering the increased inactivation of ALP at higher temperatures, the total active ALP (the encapsulated ALP ( $A_C$ ) is compared (as a ratio) to ALP in the supernatant ( $A_S$ ) + encapsulated ALP ( $A_C$ )). It can be noticed that this value ( $A_C/A_C+A_S$ ) increased from  $30^\circ\text{C}$  to  $40^\circ\text{C}$  and remains constant at  $50^\circ\text{C}$ . This indicates a possibility that encapsulation protects the enzyme against temperature induced inactivation.

### **Conclusion**

In conclusion, active enzymes alkaline phosphatase (ALP) have been encapsulated into thermally shrunk polyelectrolyte multilayer capsules templated on  $\text{CaCO}_3$  microparticles. *In situ* monitoring of capsule shrinking has been conducted by a confocal laser scanning microscope, while AFM was used to study profiles of capsules with encapsulated enzymes. Substantially thicker (almost two times comparing the maximum height) capsules, have been obtained after shrinkage. An important application of polyelectrolyte multilayer capsules, enzyme encapsulation was carried out yielding a novel procedure for heat-processing of enzymes, which maintained their activity upon encapsulation. Optimal temperature has been found for encapsulation of enzymes ( $42^\circ\text{C}$ ), and it is situated just above the glass transition temperature of  $\sim 40^\circ\text{C}$  of the used polyelectrolyte pair (PDADMAC/PSS). Enzyme activity in capsules shrunk at the optimal temperature is approximately four times higher than that measured upon exposure to  $30^\circ\text{C}$  or upon encapsulation at  $50^\circ\text{C}$ . An important application of polyelectrolyte multilayer capsules, i.e. enzyme encapsulation, was proven yielding a novel

procedure for temperature-based encapsulation of enzymes keeping their catalytic bioactivity to a high value.

## Experimental Section

*Fabrication of capsules.* Multilayer capsules were synthesized by sequential absorption of electrostatically interacting oppositely charged polymer pair (PDADMAC/PSS). In detail, excess of 2 mg/mL positively charged polymer solution in 0.5 M NaCl was added to templates, CaCO<sub>3</sub> particles, which were fabricated by the method reported previously (10.1039/c7cp07836f) (briefly, 0.3 M of sodium carbonate is added to 0.3 M of calcium chloride upon a rigorous stirring. Subsequently, the particles are collected from the solution and cleaned with water by centrifugation). The mixture was treated with ultrasound for 10 seconds, then incubated for 10 minutes. Then, it was washed three times with water. Subsequently, the second layer was constructed using the negatively charged polymer solution. The above process was repeated 4 times to generate PEM capsules of (PDADMAC/PSS)<sub>4</sub>. Ethylenediaminetetraacetic acid (EDTA) solutions was used to remove the sacrificial CaCO<sub>3</sub> core to obtain the hollow capsules.

*Fluorescence microscopy investigation of the volume shrinkage.* To assess the volume shrinkage by temperature increase, capsules were imaged using fluorescence microscopy. Images were made on a Nikon TE2000 (automated inverted microscope) using a sensitive digital sCMOS camera (Hamamatsu Orca-fusion C14440-2UP). The inclusion of TRITC polymer in the shell of the capsule allows to precisely measure the diameter of the particles at increasing temperatures. This diameter is used in turn to calculate the volume changes of the capsule.

*AFM experiments.* In order to visualise the capsules before and after shrinking with AFM, the capsules were air dried on a coverslip. The nanowizard 4™ (JPK bioAFM, Bruker) was used to obtain images of the samples in air, using QI-mode©. The probe used in these imaging measurements is the AIO (Budgetsensors), on this chip a cantilever with a spring constant of 7.4 N/m was used, this cantilever has a tip radius of <10 nm. Image processing and roughness calculation was performed in the software provided by the manufacturer (JPK data processing



software). In order to determine the capsule density, the 2D area of the capsules weight divided it by the maximum height per capsules (10 per condition). The ratio of area over height gives an approximation of the density.

*Enzyme activity measurements.* Enzyme activity of ALP was measured by a colorimetric reaction between ALP and the substrate p-NPP (p-nitrophenylphosphate). The speed of this reaction can be assessed with a spectrophotometer by measuring the absorbance change at 405 nm in a plate reader (Tecan, Infinite 200Pro). To correlate the speed of reaction to the amount of ALP in the sample, a standard curve was established using multiple concentrations of ALP assessed together with 5 mM of ALP substrate (p-NPP) in a 0.5 M solution of ALP buffer. The same reaction solution was used to determine the temperature stability of ALP and activity of the encapsulated ALP. Encapsulation of ALP was performed by combining a 100  $\mu$ L of a 1 mg/mL ALP solution with 100  $\mu$ L of capsules (containing approximately  $30E+06$  capsules). These two solutions were subsequently incubated during one hour at the predetermined temperature. After this hour the ALP/capsule mixtures were centrifuged twice and the enzyme activity was measured in both the supernatant as in the capsule fraction, in order to determine the amount of encapsulated active ALP.

#### Acknowledgements

We thank BOF UGent (01IO3618, BOF14/IOP/003, BAS094-18), FWO Flanders (G043219, 1524618N), and ERA-Net RusPlus for support. JL thanks the support of China Scholarship Council (CSC). BVP is a post-doctoral fellow of FWO. DV thanks SPF 2019/20 grant from NTU.

Received: ((will be filled in by the editorial staff))

Revised: ((will be filled in by the editorial staff))

Published online: ((will be filled in by the editorial staff))

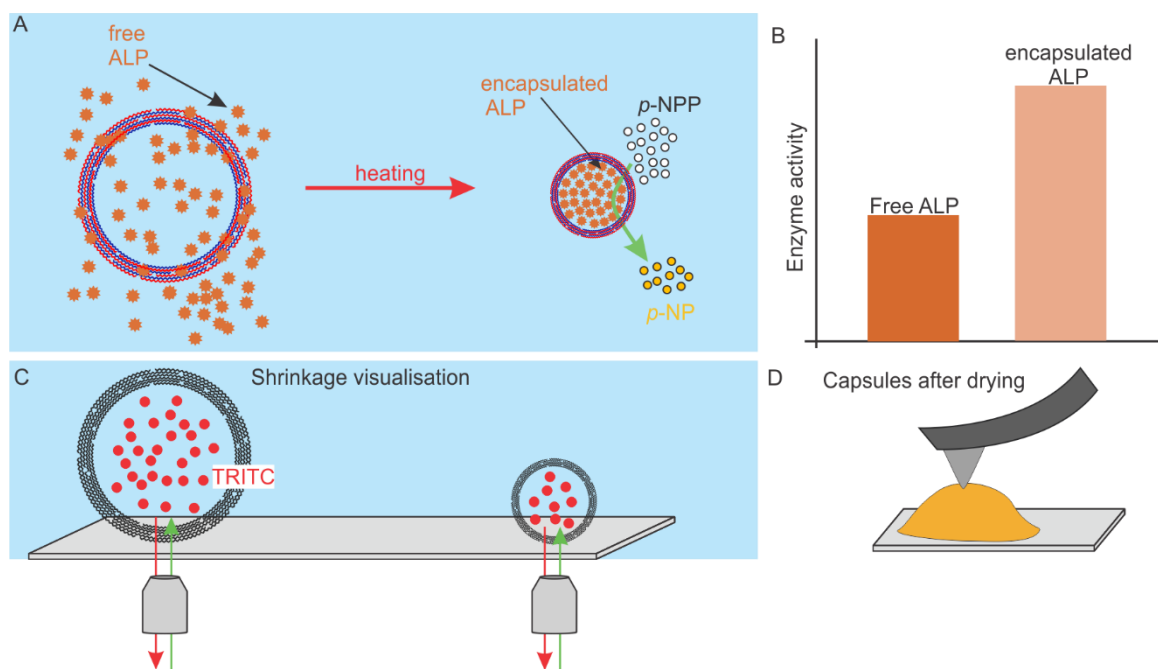


**Figure 1.** Schematics depicting the course of experiments: an enzyme (ALP) has been encapsulated by a thermally shrunk process (A); in situ investigation of enzyme activity of microcapsules (B). The thermal shrinking process of capsules is characterized by: (C) a confocal scanning laser microscope (in situ size reduction); and (D) AFM (atomic force microscope) revealing the thickness of capsules before and after shrinking.

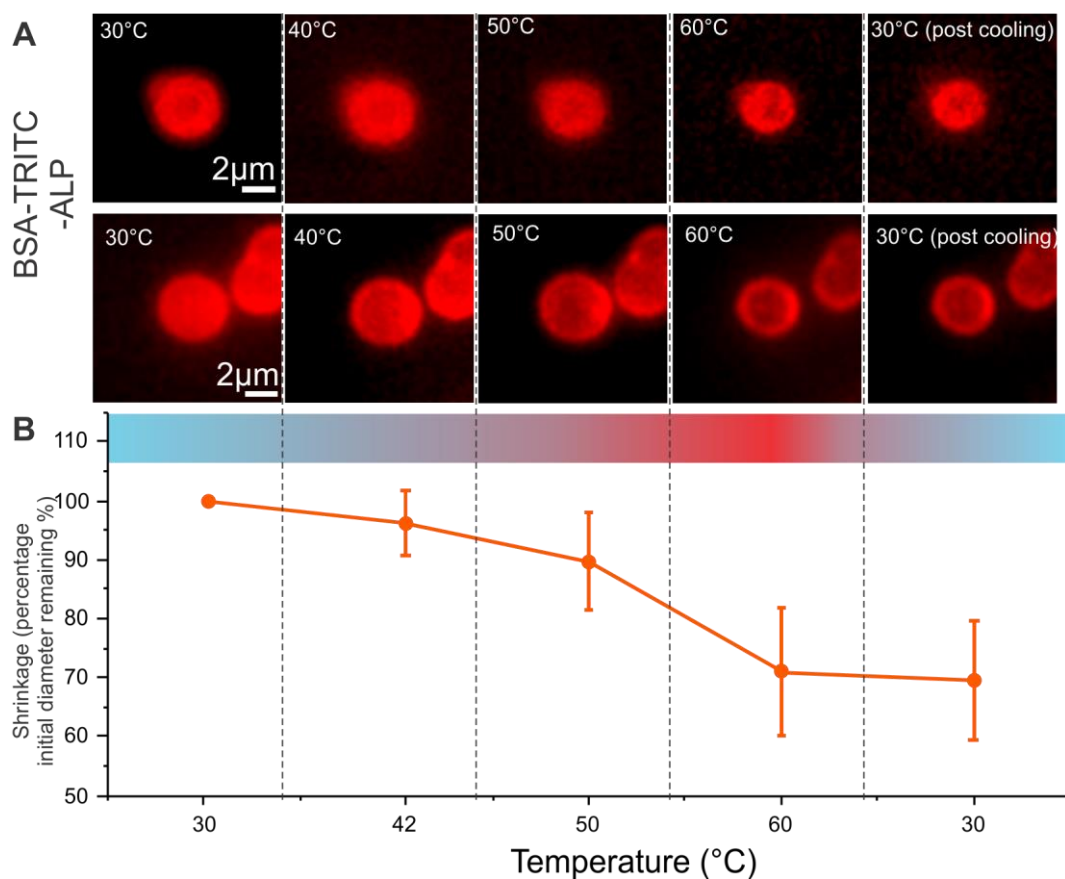


**Figure 2.** Decrease of the size of capsules upon heat-shrinking. The procedure was monitored in situ using a confocal laser scanning microscope (A). Monitoring of the diameter decrease of capsules upon shrinking (B).

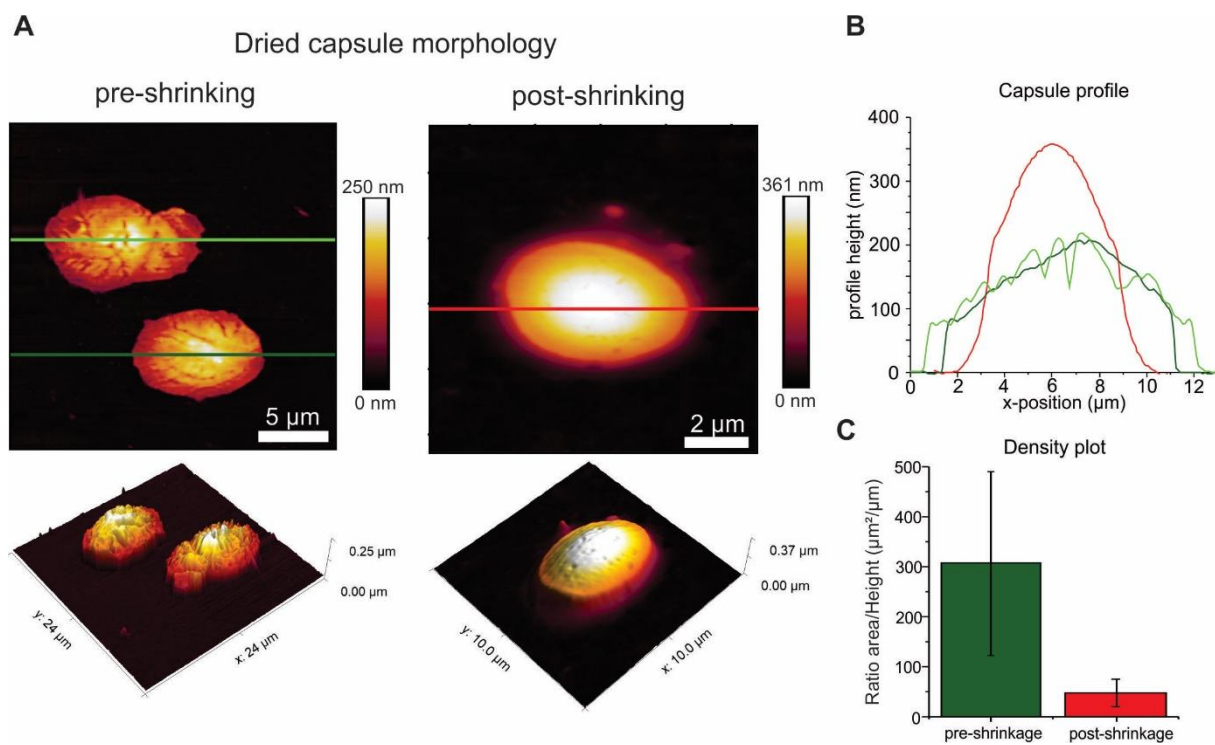


**Figure 3.** (A) Monitoring of the volume change of capsules upon cooling down to 30 degrees. (B) Height profiles as imaged by AFM in the panel (A). (C) The ratio of the area to height for pre-shrunk and post-shrunk capsules.

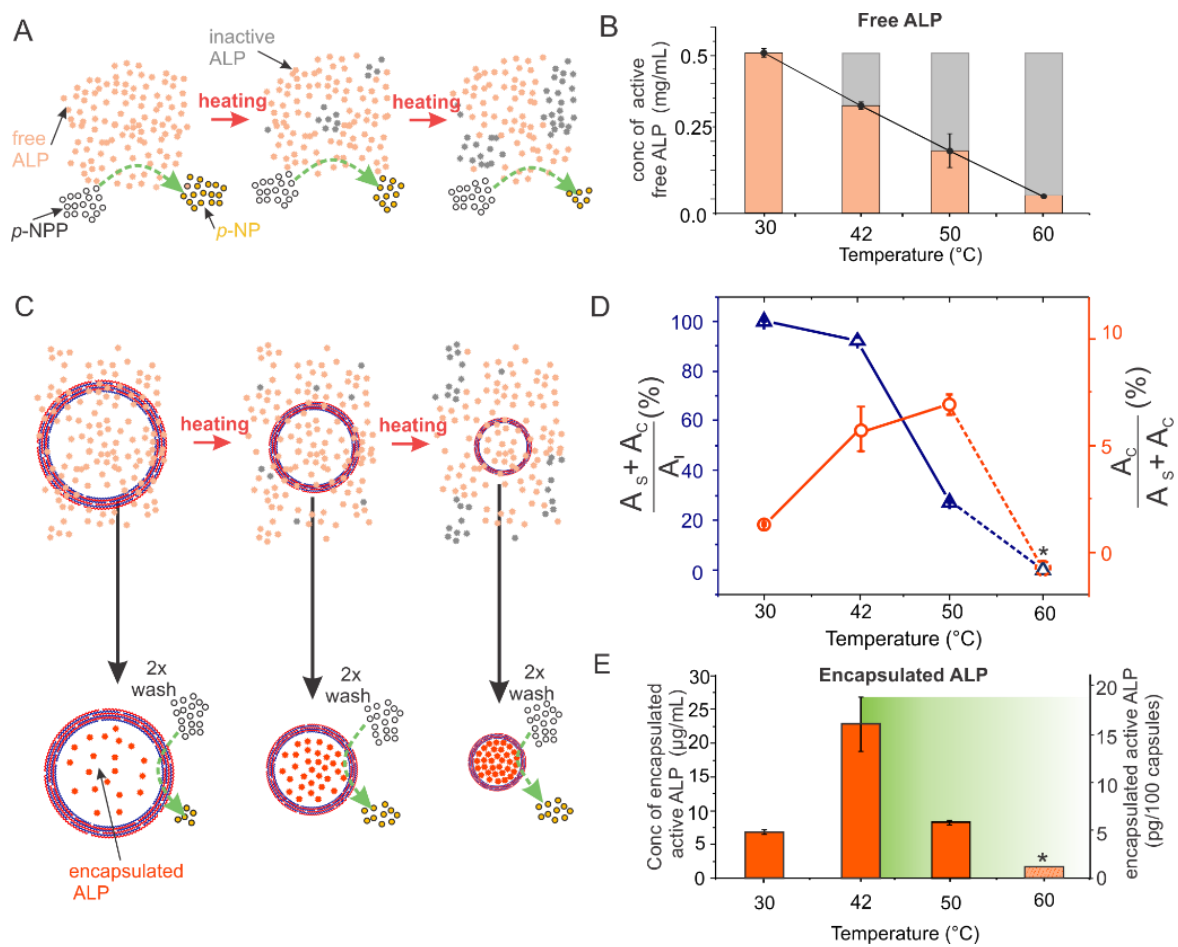


**Figure 4.** (A) Schematic of the control experiment of deactivating ALP (grey dots) shown together with active ALP (orange dots) upon exposure to elevated temperatures. (B) Reduction of the active free ALP (no encapsulation) after exposing to elevated temperatures (the initial ALP concentration is 0.5 mg/mL). (C) Schematics of encapsulation of ALP into capsules upon exposure to elevated temperatures. (D) Comparison of the total active ALP (blue) ( $A_s$ = activity ALP in supernatant,  $A_c$ = activity encapsulated ALP,  $A_i$  = initial activity of ALP) to the percentage of active ALP present inside the capsules, after heating (orange). (E) Concentration of active ALP that is encapsulated due to shrinkage of the capsules. (\*indicates that the value was lower than the detection limit in the calibration curve i.e. 0.0001 mg/mL). The window for thermal encapsulation is shown in the background in green color with a gradient.

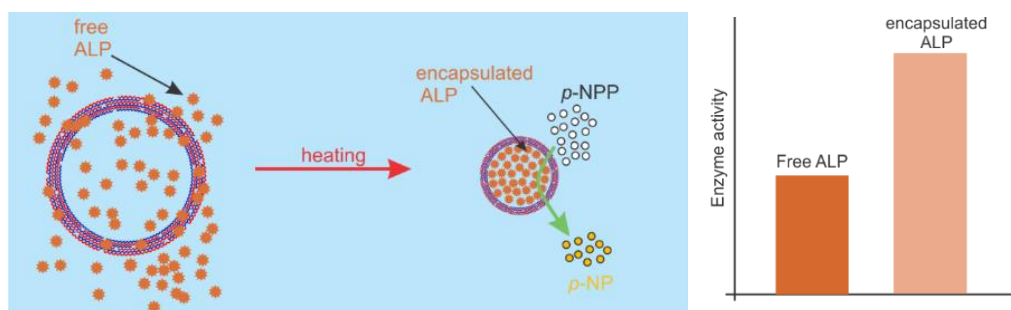
**Title:** Temperature “window” for encapsulation of enzymes into thermally shrunk,  $\text{CaCO}_3$  templated polyelectrolyte multilayer capsules

Active enzymes are encapsulated into polyelectrolyte multilayer capsules templated on calcium carbonate particles. Optimal temperature for encapsulation and preservation of enzyme activity is found.

**Keyword:** Enzyme activity in capsules

Louis Van der Meeren\*, Ji Lie, Manfred Konrad, Andre G. Skirtach, Dmitry Volodkin, Bogdan V. Parakhonskiy

**Temperature “window” for encapsulation of enzymes into thermally shrunk,  $\text{CaCO}_3$  templated polyelectrolyte multilayer capsules**



ToC figure

## References:

- [1] Mihaela Delcea, Helmuth Möhwald, André G. Skirtach, *Adv. Drug Deliv. Rev.* **2011**, *63*, 730.
- [2] Katsuhiko Ariga, Qingmin Ji, Jonathan P. Hill, "Enzyme-Encapsulated Layer-by-Layer Assemblies: Current Status and Challenges Toward Ultimate Nanodevices", in *Modern Techniques for Nano- and Microreactors/-Reactions*, F. Caruso, Ed., Springer-Verlag Berlin, Berlin, **2010**, p. 51.
- [3] Suman R. Nayak, Michael J. McShane, *J. Biomed. Nanotechnol.* **2007**, *3*, 170.
- [4] Nadezda G. Balabushevich, Olga P. Tiourina, Dmitry V. Volodkin, Natalia I. Larionova, Gleb B. Sukhorukov, *Biomacromolecules* **2003**, *4*, 1191.
- [5] Paul Rouster, Mathieu Dondelinger, Moreno Galleni, Bernard Nysten, Alain M. Jonas, Karine Glinel, *Colloids Surfaces B Biointerfaces* **2019**, *178*, 508.
- [6] Sylvia T. Gunawan, Kang Liang, Georgina K. Such, Angus P. R. Johnston, Melissa K. M. Leung, Jiwei Cui, Frank Caruso, *Small* **2014**, *10*, n/a.
- [7] Rohit Ghan, Tatsiana Shutava, Amish Patel, Vijay T. John, Yuri Lvov, *Macromolecules* **2004**, *37*, 4519.
- [8] Christos S. Karamitros, Alexey M. Yashchenok, Helmuth Möhwald, Andre G. Skirtach, Manfred Konrad, *Biomacromolecules* **2013**, *14*, 4398.
- [9] Jiwei Cui, Martin P. van Koeverden, Markus Müllner, Kristian Kempe, Frank Caruso, *Adv. Colloid Interface Sci.* **2014**, *207*, 14.
- [10] Iuliia S. Elizarova, Paul F. Luckham, *J. Colloid Interface Sci.* **2016**, *470*, 92.
- [11] Omar S. Sakr, Gerrit Borchard, *Biomacromolecules* **2013**, *14*, 2117.
- [12] Pascal K. Harimech, Raimo Hartmann, Joanna Rejman, Pablo Del Pino, Pilar Rivera-Gil, Wolfgang J. Parak, *J. Mater. Chem. B* **2015**, *3*, 2801.
- [13] Louis Van der Meeren, Jie Li, Bogdan V. Parakhonskiy, Dmitri V. Krysko, Andre G. Skirtach, *Anal. Bioanal. Chem.* **2020**, *1*, doi:10.1007/s00216-020-02428-8.
- [14] Lyubov I. Kazakova, Lyudmila I. Shabarchina, Gleb B. Sukhorukov, *Phys. Chem. Chem. Phys.* **2011**, *13*, 11110.
- [15] Weijun Tong, Xiaoxue Song, Changyou Gao, *Chem. Soc. Rev.* **2012**, *41*, 6103.
- [16] Loretta Laureana Del Mercato, Marzia Maria Ferraro, Francesca Baldassarre, Serena Mancarella, Valentina Greco, Ross Rinaldi, Stefano Leporatti, *Adv. Colloid Interface Sci.* **2014**, *207*, 139.
- [17] Andrea Belluati, Ioana Craciun, Juan Liu, Cornelia G. Palivan, *Biomacromolecules* **2018**, *19*, 4023.
- [18] Mihaela Delcea, Alexey Yashchenok, Kristina Videnova, Oliver Kreft, Helmuth Möhwald, Andre G. Skirtach, *Macromol. Biosci.* **2010**, *10*, n/a.
- [19] Hans Bäuml, Radostina Georgieva, *Biomacromolecules* **2010**, *11*, 1480.
- [20] Matias J. Cardoso, Sofia G. Caridade, Rui R. Costa, João F. Mano, *Biomacromolecules* **2016**, *17*, 1347.
- [21] Irina Marchenko, Alexey Yashchenok, Tatiana Borodina, Tatiana Bukreeva, Manfred Konrad, Helmuth Möhwald, Andre Skirtach, *J. Control. Release* **2012**, *162*, 599.
- [22] Karen Köhler, Gleb B. Sukhorukov, *Adv. Funct. Mater.* **2007**, *17*, 2053.
- [23] R. Steitz, V. Leiner, K. Tauer, V. Khrenov, R. V. Klitzing, *Appl. Phys. A Mater. Sci. Process.* **2002**, *74*, s519.
- [24] Yiming Lu, Aliaksandr Zhuk, Li Xu, Xing Liang, Eugenia Kharlampieva, Svetlana A. Sukhishvili, *Soft Matter* **2013**, *9*, 5464.
- [25] Dmitry Volodkin, *Adv. Colloid Interface Sci.* **2014**, *207*, 306.
- [26] Daria B. Trushina, Tatiana V. Bukreeva, Tatiana N. Borodina, Daria D. Belova, Sergei Belyakov, Maria N. Antipina, *Colloids Surfaces B Biointerfaces* **2018**, *170*, 312.
- [27] Alexey V. Ermakov, Olga A. Inozemtseva, Dmitry A. Gorin, Gleb B. Sukhorukov, Sergei Belyakov, Maria N. Antipina, *Macromol. Rapid Commun.* **2019**, *40*, 1800200.

- [28] Melissa Cocquyt, *Submitt.* **2016** **2016**.
- [29] Karen Köhler, Helmuth Möhwald, Gleb B. Sukhorukov, *J. Phys. Chem. B* **2006**, *110*, 24002.
- [30] Jingcheng Fu, Rachel L. Abbett, Hadi M. Fares, Joseph B. Schlenoff, *ACS Macro Lett.* **2017**, *6*, 1114.
- [31] Yanpu Zhang, Piotr Batys, Joshua T. O'Neal, Fei Li, Maria Sammalkorpi, Jodie L. Lutkenhaus, *ACS Cent. Sci.* **2018**, *4*, 638.
- [32] Rabih F. Shamoun, Haifa H. Hariri, Ramy A. Ghostine, Joseph B. Schlenoff, *Macromolecules* **2012**, *45*, 9759.
- [33] Joshua T. O'Neal, Kathryn G. Wilcox, Yanpu Zhang, Ian M. George, Jodie L. Lutkenhaus, *J. Chem. Phys.* **2018**, *149*, 163317.
- [34] Andre G. Skirtach, Almudena Muñoz Javier, Oliver Kreft, Karen Köhler, Alicia Piera Alberola, Helmuth Möhwald, Wolfgang J. Parak, Gleb B. Sukhorukov, *Angew. Chemie Int. Ed.* **2006**, *45*, 4612.
- [35] Renate Mueller, Karen Köhler, Richard Weinkamer, Gleb Sukhorukov, Andreas Fery, *Macromolecules* **2005**, *38*, 9766.
- [36] Raghavendra Palankar, Bat El Pinchasik, Stephan Schmidt, Bruno G. De Geest, Andreas Fery, Helmuth Möhwald, André G. Skirtach, Mihaela Delcea, *J. Mater. Chem. B* **2013**, *1*, 1175.
- [37] Dmitry V. Volodkin, Alexander I. Petrov, Michelle Prevot, Gleb B. Sukhorukov, *Langmuir* **2004**, *20*, 3398.



## Supporting Information

### **Temperature “window” for encapsulation of enzymes into thermally shrunk, CaCO<sub>3</sub> templated polyelectrolyte multilayer capsules**

*Louis Van der Meeren\**, Jie Li, Manfred Konrad, Andre G. Skirtach, Dmitry Volodkin, Bogdan V. Parakhonskiy

L. Van der Meeren, J. Li, A.G. Skirtach, B. V. Parakhonskiy  
Department of Biotechnology, Ghent University, 9000 Ghent, Belgium

E-mail: [Louis.VanderMeeren@UGent.be](mailto:Louis.VanderMeeren@UGent.be)

M. Konrad

Max Planck Institute for Biophysical Chemistry, 37077 Göttingen, Germany

D. Volodkin

School of Science and Technology, Nottingham Trent University, Nottingham NG11 8NS, U.K.

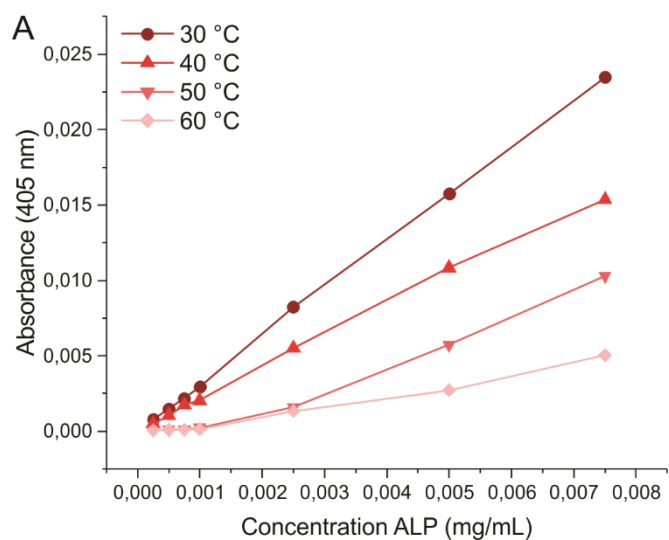


**Figure S1:** The calibration curve correlating the concentration of ALP with the increase of absorbance over time during the enzymatic reactions. Different colours indicate the multiple temperatures, at which calibration curves were calculated.

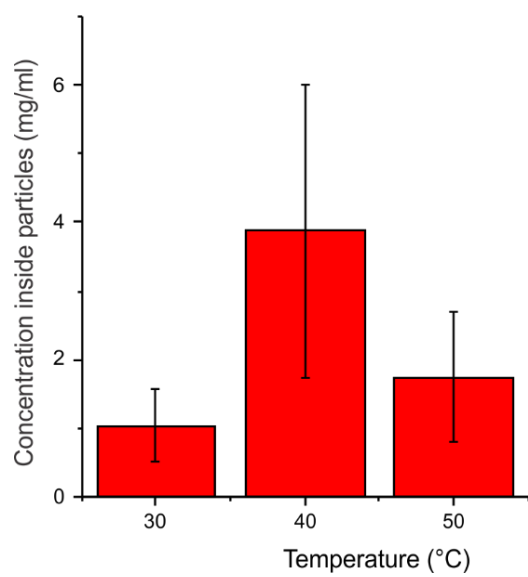


**Figure S2:** Bar graph which indicates the concentration of active ALP measured inside the particles, error bars indicate the standard deviation.